

Spin coherence and Humpty-Dumpty. III. The effects of observation

Marlan O. Scully, Berthold-Georg Englert,* and Julian Schwinger†

Max-Planck-Institut für Quantenoptik, D-8046 Garching, Federal Republic of Germany
and Center for Advanced Studies and Department of Physics and Astronomy, University of New Mexico,
Albuquerque, New Mexico 87131

(Received 28 October 1988)

In recent work a Stern-Gerlach interferometer (SGI) was considered in which a polarized beam of spin- $\frac{1}{2}$ particles is split by a Stern-Gerlach apparatus into two partial beams, and then subsequent Stern-Gerlach deflecting magnets are used to reconstitute these two beams into one. In these studies it was shown that when such a coherent polarized beam passed through a SGI, some spin coherence is inevitably lost. In this regard, folk wisdom concerning irreversibility provides something of a guide to the present problem, since we all know that when Humpty-Dumpty had his great fall nobody could put him together again. In the present paper we consider the fate of our spin- $\frac{1}{2}$ Humpty-Dumpty when a detector is present that is sensitive to the passage of particles along one trajectory, but not the other. It is not surprising that coherence is destroyed as soon as one is able to tell along which path the atom traveled. However, there seems to be no general agreement about the mechanism of coherence loss. Our conclusion is that the loss of coherence in measurements on quantum systems can always be traced to the dynamics of correlations between the measuring apparatus and the system being observed.

I. INTRODUCTION

A. Wigner's Stern-Gerlach interferometer

In a seminal paper, Wigner¹ discussed the separation of an x -polarized beam of spin- $\frac{1}{2}$ atoms into two z -polarized beams (spin \uparrow and \downarrow) by a Stern-Gerlach² apparatus (SGA), and the spin state which would result if one subsequently merged the two beams, as in Fig. 1. We note that this sequence of beam separation, propagation and recombination is analogous to an optical interferometer. Thus we will speak of the experimental arrangement of Fig. 1 as a Stern-Gerlach interferometer (SGI).

The question put by Wigner is: Can the reconstituted beam be in a coherent, x -polarized spin state or is the coherence destroyed by the separation and recombination? To put the issue and problem in more operational and physical terms, consider Fig. 2. There we have indicated a final SGA oriented along the x axis. If the emerging beam is x polarized, i.e., if

$$\langle \sigma_x \rangle = 1 \tag{1}$$

or

$$\rho_{\text{spin}} = \frac{1}{2}(1 + \sigma_x), \tag{2}$$

then all of the particles will be deflected in the $+x$ direction. However, if the beam is unpolarized, i.e., if

$$\rho_{\text{spin}} = \frac{1}{2} \tag{3}$$

and

$$\langle \sigma_x \rangle = 0, \tag{4}$$

then half of the atoms will be deflected in the $+x$ and half in the $-x$ direction. In principle, then, the two possibilities can be distinguished.

One reason for our interest in the question is that thoughtful physicists have given us different answers to Wigner's question. Some say: "Yea, the output of the SGI will be coherent since the different parts of the SGI involve magnetic fields which are reversed in subsequent sections of the apparatus, and this is equivalent to time reversal." Other say: "Nay, the output of the SGI will be totally incoherent since the wave packets describing the center-of-mass motion will be of finite extent, so that the atom will probe different magnetic fields at different points in the packet; thus there must be a 'scrambling' of the phase of the spin- $\frac{1}{2}$ atom."

Therefore, we have been stimulated to work out a detailed analysis of the SGI, which is the subject of two recent papers about spin coherence and Humpty-Dumpty. We all know that after Humpty-Dumpty's great fall (see Ref. 3) no one could put him together again. In those papers we took up the more modest challenge of trying to put the two partial beams of a SGA back together with

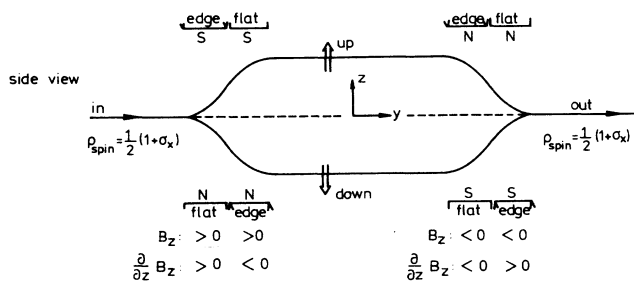
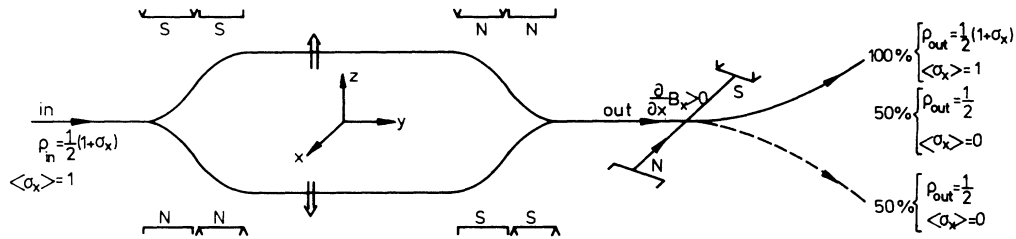


FIG. 1. Side view of the Stern-Gerlach interferometer.

FIG. 2. SGI with SGA for final σ_x measurements.

such precision that the original spin state was recovered.

In the first paper³ about spin coherence in SGI's (I), we found that the spin coherence is largely recovered if the magnetic fields are controlled to a sufficiently great accuracy. In this sense our "yea-say" friends are right, spin coherence is (in principle) maintained. However, in another paper⁴ (II) in which we solved the quantum-mechanical problem more completely (involving a quantum treatment of the center-of-mass motion, and that requires a realistic magnetic field), we found that some loss of coherence is inevitable. In this sense our "nay-say" friends may claim some support.

Although the reconstituted beam will, in principle, show some loss of coherence (there will be some inevitable cracks left in Humpty-Dumpty's shell), we can come close enough to recovering spin coherence so that, for the purposes of the present paper, we can and will pretend that the original spin state is recovered.

Another type of beam recombination has been accomplished in recent neutron interferometric experiments.⁵ In these experiments it was shown that two partial beams (again spin \uparrow and \downarrow) can be combined to produce an x -polarized beam. Suffice it to say that both theoretical and experimental studies show that the reconstitution of two partial beams can in principle (SGI) and in practice (neutron interferometer) produce a coherent x -polarized spin state.

The objective of the present paper is to understand what happens to spin coherence when a "which path" (German: *welcher Weg*) detector is put into one arm—the upper path, say—of the SGI. Whereas it would generally be agreed that spin coherence is destroyed, as soon as one is able to tell along which one of the two paths the spin $-\frac{1}{2}$ atom traveled through the SGI, the question, *how* this loss of coherence comes about, is answered in different ways. Some insist that in the process of measurement the system under observation is always affected in a form analogous to the recoil acquired by the scattering of the photon in "Heisenberg's⁶ microscope," that is, the spatial properties of the observed system are changed significantly. Others point to the large number of degrees of freedom in the macroscopic measuring apparatus, which implies—so they argue—an irreversible change responsible for the loss of coherence.

These explanations may be relevant in particular experimental situations. More generally put, we support the view that the loss of coherence in measurements on

quantum systems can always be traced to correlations between the (relevant) degrees of freedom of the measuring apparatus and the system being observed. The correlations are built up in the course of the measurement, and their temporal evolution is correctly described by quantum mechanics. In particular, one need not resort to invoking the notions of "state reduction" or the "collapse of the wave function" as *dei ex machina*, whose dynamical properties are allegedly outside the framework of quantum mechanics.

B. Adding a recoil *welcher Weg* detector

Let us begin our survey of possible *welcher Weg* detectors by a brief discussion of one of the simplest. A detector *particle* is put into the upper beam path; it scatters the spin- $\frac{1}{2}$ atom when they encounter each other, and the resulting observed momentum change of the particle signifies that the atom went along the upper path. This is a detector of the Heisenberg-microscope type. For it to work, the momentum Δp , transferred to the particle during the collision, must be significantly larger than the spread of momentum δp of the particle before the collision; otherwise we cannot tell whether a collision happened at all. Since the spread in position δz of the particle and the atom are of the same size before the collision (this is the meaning of "putting the particle into the upper beam path"), the corresponding momentum spreads are comparable as well. Momentum conservation implies that the change of momentum of the atom equals $-\Delta p$, so that its momentum is also changed significantly. Now recall that the magnetic fields in the SGI are set such that, in the absence of the detector particle, the two partial beams are well focused and spin coherence (largely) regained. According to I, this requires that the net momentum transfer by the SGI to the atom (after recombination) is negligible compared to the momentum spread δp . In contrast, when the particle has suffered a *detectable* momentum change, then the atomic momentum is also changed significantly and I tells us that *spin coherence is lost*. On the other hand, an *insignificant* recoil of the detector particle implies an equally negligible momentum transfer to the atom, under which condition *spin coherence is not lost*. Here we are unable to tell along which path the atom went. In other words, if we count only those atoms for which the detector particle is scattered out of the beam path, we will find

the final spin density operator to be $\rho_{\text{spin}} = \frac{1}{2}$; if we select, however, those atoms for which the momentum transfer to the particle is not noticeable, the outcome is $\rho_{\text{spin}} = \frac{1}{2}(1 + \sigma_x)$, ideally.

C. Adding a toy (two-level atom) *welcher Weg* detector

In a previous extension⁷ of Wigner’s SGI study a *welcher Weg* detector was added to the problem such that it was sensitive to atoms passing in its locale, see Fig. 3. This early work, co-authored by one of us, involved a toy detector simplified to the point that it was taken as a two-level atom with states *a* (excited) and *b* (ground).

The system-detector wave function is then a four-component object,

$$\Psi(\mathbf{r}, t) = \begin{pmatrix} \psi_{a\uparrow}(\mathbf{r}, t) \\ \psi_{a\downarrow}(\mathbf{r}, t) \\ \psi_{b\uparrow}(\mathbf{r}, t) \\ \psi_{b\downarrow}(\mathbf{r}, t) \end{pmatrix} = \begin{pmatrix} \text{detector excited and spin up} \\ \text{detector excited and spin down} \\ \text{detector not excited and spin up} \\ \text{detector not excited and spin down} \end{pmatrix}. \tag{5}$$

The detector was designed so as to respond to the probability that the atom is found at \mathbf{r}_d , the detector’s position, and their interaction was written as

$$V = g\delta(\mathbf{r} - \mathbf{r}_d)(|a\rangle\langle b| + |b\rangle\langle a|)(|\uparrow\rangle\langle\uparrow| + |\downarrow\rangle\langle\downarrow|). \tag{6}$$

Evidently there will be recoil effects produced by the δ -function potential in addition to changes of the internal detector state. However, in that early study, it was noticed that spin coherence was destroyed owing to correlations between the detector and the spin- $\frac{1}{2}$ atom, independent of scattering effects on the center-of-mass part of wave function. The notion that observation produces correlation, which in turn leads to incoherence, was regarded as the main point rather than the particular effect of recoil. This is not satisfactory for several reasons.

- (a) Since the δ -function interaction is so highly localized, the neglect of scattering is unphysical.
- (b) While it is true that the atom-detector correlation

destroys spin coherence, recoil effects will “do the job” anyway. So one might wonder whether in all realistic experiments the ever-present recoil effects would suffice to destroy coherence. This raises the question of whether correlations referring to internal degrees of freedom are only of secondary interest.

- (c) Over-idealized models are not good guides to suggesting experiments.

It is a purpose of the present paper to reexamine the previous arguments and to propose and analyze a micromaser *welcher Weg* detector which does *not* scatter the spin- $\frac{1}{2}$ atoms to a significant extent. An essential difference between the previous toy detector and the more realistic new one is that we now use a much less localized interaction.

D. Adding a micromaser *welcher Weg* detector

Here we present the idea of the micromaser *welcher Weg* detector; the detailed analysis is given in Sec. II. Let us begin by recalling that the SGI of Fig. 1 pretends that the emerging atoms have spin properties identical with those of the entering ones. In other words, the spin operator $\sigma(t_f)$ at the final time t_f , safely after the atom has left the SGI, equals the initial $\sigma(t_i)$, where the initial time t_i is safely before the atom entered the SGI:

$$\sigma(t_f) = \sigma(t_i). \tag{7}$$

This is equivalent to saying that the unitary evolution operator $U_{\text{SGI}}(t_i, t_f)$ affects only the spatial operators describing the center-of-mass motion, and, since the SGI ideally does neither displace the atom nor transfer momentum, we have

$$U_{\text{SGI}}(t_i, t_f) = \exp\left[-\frac{i}{\hbar} \frac{[\mathbf{p}(t_i)]^2}{2m}(t_f - t_i)\right], \tag{8}$$

which says that after the partial beams have been recombined, the wave function does not differ from that resulting from the free motion of the atom.

Now we add two micromaser cavities to the upper beam flight path as depicted in Fig. 4. The single-mode maser fields are prepared such that the probability that a spin-up atom entering cavity 1 is spin down between the cavities and spin up again after leaving cavity 2 is practically equal to unity. Since only the upper partial beam runs through the cavities, the evolution operator describ-

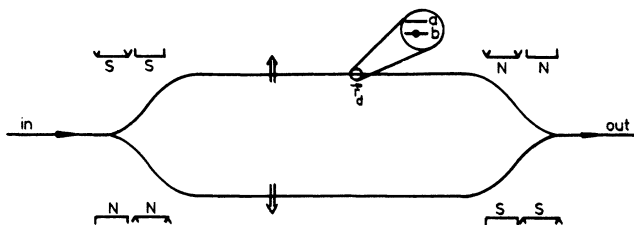


FIG. 3. SGI with two-level atom *welcher Weg* detector.

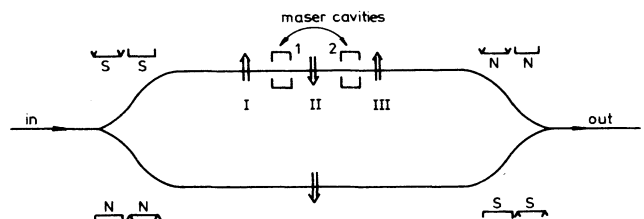


FIG. 4. SGI with micromaser *welcher Weg* detector.

ing the SGI with the cavities has the structure

$$U(t_i, t_f) = U_{\text{SGI}}(t_i, t_f) \left[\frac{1 + \sigma_z(t_i)}{2} U_{\text{cav}}^{(\uparrow)}(t_i, t_f) + \frac{1 - \sigma_z(t_i)}{2} U_{\text{cav}}^{(\downarrow)}(t_i, t_f) \right], \quad (9)$$

where $U_{\text{cav}}^{(\downarrow)}$ refers (essentially) to the free evolution of the cavity fields, whereas $U_{\text{cav}}^{(\uparrow)}$ accounts also for the interaction of the upper-beam atoms with the cavities.

As always, we take the entering atoms to be in the $\sigma'_x(t_i) = 1$ state. Since a net Larmor precession may render the emerging beam polarized in any direction in the x, y plane, the magnitude of the expectation value $\langle \sigma_x(t_f) \rangle$ alone is not a good measure of spin coherence. As in II, we use the number

$$C \equiv [\langle \sigma_x(t_f) \rangle^2 + \langle \sigma_y(t_f) \rangle^2]^{1/2} = | \langle \sigma_x(t_f) + i \sigma_y(t_f) \rangle |, \quad (10)$$

instead. As shown in Sec. II below, one finds

$$C = | \langle U^{-1}(t_i, t_f) [\sigma_x(t_i) + i \sigma_y(t_i)] U(t_i, t_f) \rangle | \cong | \langle a_1(t_i) \rangle \langle a_2^\dagger(t_i) \rangle | / \sqrt{N_1 N_2}, \quad (11)$$

where a_j (a_j^\dagger) are the standard annihilation (creation) operators of the photons in the j th cavity, and

$$N_j = \langle a_j^\dagger(t_i) a_j(t_i) \rangle, \quad j = 1, 2 \quad (12)$$

are the average photon numbers in the cavities, initially. The setup of Fig. 4 works in the desired way if the N_j 's are certain (very) large numbers and the uncertainties

$$\delta N_j \equiv \{ \langle [a_j^\dagger(t_i) a_j(t_i) - N_j]^2 \rangle \}^{1/2}, \quad j = 1, 2 \quad (13)$$

are small compared to the average values,

$$\delta N_j \ll N_j, \quad j = 1, 2. \quad (14)$$

Under these conditions, the result given in (11) is a very good approximation.

Now consider two extreme situations: (a) the cavities are prepared in eigenstates of $a_1(t_i)$ and $a_2(t_i)$; (b) they are prepared in eigenstates of $a_1^\dagger(t_i) a_1(t_i)$ and $a_2^\dagger(t_i) a_2(t_i)$. For (a), we have so-called *coherent states* of the maser fields which, because N_1 and N_2 are large numbers, are classical states of the electromagnetic field. Further, here

$$N_j = \langle a_j^\dagger(t_i) \rangle \langle a_j(t_i) \rangle = | \langle a_j(t_i) \rangle |^2, \quad j = 1, 2 \quad (15)$$

so that (11) gives

$$C \cong 1. \quad (16)$$

In contrast, the so-called *number states* of (b) have the

$$\frac{1}{\sqrt{2}} (|N_1, N_2, \downarrow, t_f\rangle e^{i\phi/2} - |N_1 + 1, N_2 - 1, \uparrow, t_f\rangle e^{-i\phi/2}) e^{-i(N_1 + N_2)\beta}, \quad (20)$$

where the photon quantum numbers are $\langle a_j^\dagger a_j \rangle'$ at $t = t_f$, and ϕ, β are presently irrelevant phases. The spin-up and

property

$$\langle a_j(t_i) \rangle = \langle a_j^\dagger(t_i) \rangle = 0, \quad (17)$$

which used in (11) produces

$$C \cong 0. \quad (18)$$

Thus, classical coherent maser states preserve spin coherence, but number states destroy it.

How can that be? Have we not merely flipped the spins in the upper beam from up to down to up in both cases with no apparent net effect on the spin properties of the upper beam atoms? Yes, but there is more to it. Since the partial beams are characterized by the value of $\sigma'_z(t_i) = \pm 1$, the interaction with the cavity photons correlates the spin degree of freedom to the photon degrees of freedom. Thus the outcome of final spin measurements depends on the prepared cavity states, as expressed in Eq. (11), and vice versa: the results of measuring the values of photon operators at or after time t_f depends on the initial spin state of the atom. Consequently, which-path information is potentially available, provided the properties of the maser fields are changed in a *discernible* fashion by the interaction. It is here that the distinction between coherent states and number states enters. This is shown in two different ways in the following two paragraphs.

Consider, for instance, the count of photons in cavity 1 after the atom has traversed the apparatus. Quoting from Sec. II below we have

$$\langle a_1^\dagger(t_f) a_1(t_f) \rangle \cong N_1 + \frac{1}{2} = \frac{1}{2} N_1 + \frac{1}{2} (N_1 + 1) \quad (19)$$

for atoms with initially $\sigma'_x(t_i) = 1$. The latter decomposition exhibits the probabilities of $\frac{1}{2}$ for finding spin down or spin up, for which the photon number is unchanged or increased by 1, respectively. Now, in the coherent state one has $\delta N_1 = \sqrt{N_1}$, $\delta N_1 / N_1 = 1 / \sqrt{N_1} \ll 1$, so that when measuring $a_1^\dagger(t_f) a_1(t_f)$ the various integers between (roughly) $N_1 - \sqrt{N_1}$ and $N_1 + \sqrt{N_1}$ are found. Because this range consists of (very) many possible outcomes, a change in photon number by 1 cannot be detected; this is analogous to insufficient momentum transfer to the recoil detector of Sec. I B. In contrast, the number state has $\delta N_1 = 0$, and (19) tells us that at time t_f we will either find exactly N_1 photons or exactly $N_1 + 1$ photons, signifying spin down or spin up, respectively. Here we indeed have which-path information, and spin coherence is lost. This situation is analogous to a detectable momentum change of the recoiled particle.

The *welcher Weg* nature of these two extreme situations (number versus coherent-state preparation) is also clearly displayed upon expressing the state of the spin-photon system in terms of states referring to measurements at the final time t_f . As shown in Sec. II below, for initial number states $[(a_j^\dagger a_j)' = N_j \text{ at } t = t_i]$, we have

spin-down components are physically distinguished here, inasmuch as there is a one-to-one correspondence between spin down and final photon counts N_1, N_2 , as well as spin up and $N_1 + 1, N_2 - 1$. This signifies the correlations established by the interaction. In short, number-state preparation provides us with a good *welcher Weg* detector. In contrast to Eq. (20), cavities prepared in classical coherent states [$a_j'(t_i) = \alpha_j = \sqrt{N_j} e^{i\theta_j}$] yield

$$\frac{1}{\sqrt{2}} (|\alpha_1 e^{-i\beta}, \alpha_2 e^{-i\beta}, \downarrow, t_f\rangle e^{i\psi/2} + |\alpha_1 e^{-i\beta}, \alpha_2 e^{-i\beta}, \uparrow, t_f\rangle e^{-i\psi/2}) e^{-i(\pi + \theta_1 - \theta_2)/2} \\ = |\alpha_1 e^{-i\beta}, \alpha_2 e^{-i\beta}, (\sigma_x \cos\psi + \sigma_y \sin\psi)' = 1, t_f\rangle e^{-i(\pi + \theta_1 - \theta_2)/2}, \quad (21)$$

where the photon quantum numbers are $a_j'(t_f)$. Here the photon and spin degrees of freedom are evidently uncorrelated, and therefore we do not have a functioning *welcher Weg* detector. The net effect on the spin of the atom is a coherence preserving Larmor precession through the angle $\psi = \pi + \phi + \theta_1 - \theta_2$. Incidentally, we remark that the relative phase $\theta_1 - \theta_2$ between the two coherent states must be well controlled, which can be achieved by feeding both cavities from one external source.

Readers interested in a density operator treatment are referred to Sec. II C.

Naturally, there are situations intermediate between the two extremes of coherent states and number states. For example, if the cavities are prepared in eigenstates of the operators

$$a_j \cosh\lambda_j + a_j^\dagger \sinh\lambda_j, \quad j = 1, 2 \quad (22)$$

with (real) parameters $\lambda_{1,2}$ (these are so-called squeezed states), then one has

$$\langle a_j \rangle \langle a_j^\dagger \rangle = |\langle a_j \rangle|^2 = \langle a_j^\dagger a_j \rangle - \sinh^2\lambda_j \\ = N_j - \sinh^2\lambda_j, \quad (23)$$

and Eq. (11) gives

$$C \cong \left[1 - \frac{\sinh^2\lambda_1}{N_1} \right]^{1/2} \left[1 - \frac{\sinh^2\lambda_2}{N_2} \right]^{1/2}, \quad (24)$$

thus $0 < C < 1$ here, so that spin coherence is only partially lost.

II. MICROMASER WELCHER WEG DETECTOR

A. Effective treatment of the atom-cavity interaction

In the context of the SGI it is natural to consider *magnetic* dipole interactions between the atoms and the maser fields.⁸ The interaction energy of the atom with magnetic moment $\boldsymbol{\mu} = \mu\boldsymbol{\sigma}$ coupled to the quantized electromagnetic field of one mode in one of the cavities is

$$-\boldsymbol{\mu} \cdot \mathbf{B} = -\mu\boldsymbol{\sigma}(t) \cdot \{ \nabla \times c\sqrt{2\pi\hbar/\omega} [\mathbf{A}(\mathbf{r})a(t) \\ + \mathbf{A}^*(\mathbf{r})a^\dagger(t)] \}, \quad (25)$$

where $\hbar\omega$ is the energy per photon, $\mathbf{A}(\mathbf{r})$ is the spatial mode function, and a, a^\dagger are the photon annihilation and creation operators of the respective modes. The mode function is normalized according to

$$\int (d\mathbf{r}') \mathbf{A}^*(\mathbf{r}') \cdot \mathbf{A}(\mathbf{r}') = 1, \quad (26)$$

where the range of integration covers the volume of the cavity. The coupling (25) is *very* weak; for illustration, consider an atom with a magnetic moment equal to one Bohr magneton and a cavity of linear dimensions $L \sim c/\omega$, for which

$$\left| \mu c \left[\frac{2\pi\hbar}{\omega} \right]^{1/2} \nabla \times \mathbf{A} \right| \sim \frac{e\hbar}{m_e c} c \left[\frac{\hbar}{\omega} \right]^{1/2} L^{-5/2} \\ \sim \frac{(\hbar\omega)^2}{m_e c^2} \sqrt{\alpha}, \quad (27)$$

where m_e and e are the mass and charge of the electron, and $\alpha = e^2/\hbar c = \frac{1}{137}$ is the fine-structure constant. In a maser we have, typically, $\hbar\omega \sim 10^{-5}$ eV, which, combined with $m_e c^2 = 5 \times 10^5$ eV, gives about 10^{-16} eV for the coupling strength.

We shall now take for granted that only one mode in the cavity is highly excited, so that only this mode produces dynamical effects. Further, to achieve a substantial computational simplification, we assume that the corresponding $\mathbf{A}(\mathbf{r})$ is such that the magnetic field is circularly polarized in the x, y plane,

$$c \left[\frac{2\pi\hbar}{\omega} \right]^{1/2} \nabla \times \mathbf{A}(\mathbf{r}) = \frac{1}{2} b(\mathbf{r}) \begin{pmatrix} 1 \\ i \\ 0 \end{pmatrix}, \quad (28)$$

with real $b(\mathbf{r})$. Then (25) reads

$$-\boldsymbol{\mu} \cdot \mathbf{B} = -\frac{1}{2} \mu b(\mathbf{r}) (a\sigma_+ + a^\dagger\sigma_-), \quad (29)$$

where we encounter the spin-flip operators $\sigma_\pm = (\sigma_x \pm i\sigma_y)$.

Even with very many photons present, the interaction energy (29) will be negligible compared with the kinetic energy of the atom. As a consequence, the interaction with the maser field does not produce a significant change of the center-of-mass motion of the atom. (There is a residual displacement along the trajectory which is, however, small compared to the spread of the wave function. This and other presently irrelevant details are planned to be discussed in a separate publication.)⁹ There is also no substantial scattering of the atom by the rim of the holes through which it enters and leaves the cavities. For, owing to the macroscopic beam splitting achieved in the initial stage of the SGI, these holes can be made large compared with the beam width. On the other hand, the spread of the atomic spatial wave function is small on the scale set by the dimensions of the cavities, and therefore

the atom probes, at a given time, only a small portion of $b(\mathbf{r})$. Analogous to the treatment in I, which is justified in II, we shall therefore replace the spatial (operator) function $b(\mathbf{r})$ by its expectation value at time t , $\langle b(\mathbf{r}(t)) \rangle$, which involves the spatial properties of the atom; more precisely, this function of time refers to the center-of-mass part of the wave function of the upper beam. We have now arrived at

$$-\boldsymbol{\mu} \cdot \mathbf{B} \rightarrow -\frac{1}{2} \hbar g(t) (a \sigma_+ + a^\dagger \sigma_-) \quad (30)$$

as the effective description of the coupling to the selected cavity mode. The numerical function $g(t)$ is nonzero only while the atom is inside the cavity. As pointed out in Ref. 9, further details of $g(t)$ do not matter in the present context, so that we can take it to be constant for a total duration T , starting at $t = \tau$:

$$g(t) = \begin{cases} g & \text{for } \tau < t < \tau + T, \\ 0 & \text{otherwise.} \end{cases} \quad (31)$$

A large effect can only accumulate if the operator

$$\gamma = \frac{1}{2} (a \sigma_+ + a^\dagger \sigma_-), \quad (32)$$

appearing in the interaction energy (30), does not itself oscillate rapidly in time. Therefore, one needs an additional homogeneous, constant external magnetic field $\mathbf{B}_0 = B_0 \mathbf{e}_z$ in the region between the Stern-Gerlach magnets, the strength of which is chosen such that the energy difference $2\mu B_0$ between the spin-up and -down states equals the energy per photon of the mode. This way, the coupling is resonant and much more effective in producing spin flip.

Our Hamilton operator describing, in effect, the interaction occurring in the upper partial beam with the cavity modes now referring to both cavities, is then

$$H_{\text{eff}} = \hbar \omega (a_1^\dagger a_1 + a_2^\dagger a_2 + \frac{1}{2} \sigma_z) - \frac{1}{2} \hbar g_1(t) (a_1 \sigma_+ + a_1^\dagger \sigma_-) - \frac{1}{2} \hbar g_2(t) (a_2 \sigma_+ + a_2^\dagger \sigma_-), \quad (33)$$

where, as in (31), the time-dependent coupling constants $g_{1,2}(t)$ are nonzero only for $\tau_j < t < \tau_j + T_j$. In the sequel, we consider three instants: t_1 is before the atom enters the first cavity, t_2 is after it has left the first and before it enters the second, and t_3 is after it has left the second. That is, $t_{1,2,3}$ refer to the spatial regions I, II, III in Fig. 4, respectively. Thus we have the sequence

$$t_i < \tau_1 < \tau_1 + T_1 < t_2 < \tau_2 < \tau_2 + T_2 < t_3. \quad (34)$$

Upon introducing γ_1 and γ_2 analogous to (32) and observing the identity

$$\gamma_j^2 = a_j^\dagger a_j + \frac{1}{2} (1 + \sigma_z), \quad (35)$$

we can present H_{eff} more compactly,

$$H_{\text{eff}} = \hbar \omega (\gamma_1^2 + a_2^\dagger a_2 - \frac{1}{2}) - \hbar g_1(t) \gamma_1 - \hbar g_2(t) \gamma_2 = \hbar \omega (a_1^\dagger a_1 + \gamma_2^2 - \frac{1}{2}) - \hbar g_1(t) \gamma_1 - \hbar g_2(t) \gamma_2 \quad (36)$$

of which the first version is particularly useful when $g_2(t) = 0$, that is, for $t_1 < t < t_2$, and the second one when $g_1(t) = 0$, that is, for $t_2 < t < t_3$.

The overall evolution operator of Eq. (9) can now be computed. Details are presented in the Appendix, from which we quote the result

$$U(t_i, t_f) = U_{\text{SGI}}(t_i, t_f) \exp \left\{ -i \omega (t_f - t_i) [a_1^\dagger(t_i) a_1(t_i) + a_2^\dagger(t_i) a_2(t_i)] \right\} \exp \left[-\frac{i}{2} \phi \sigma_z(t_i) \right] \times \left[\frac{1 + \sigma_z(t_i)}{2} \exp[ig_2 T_2 \gamma_2(t_i)] \exp[ig_1 T_1 \gamma_1(t_i)] + \frac{1 - \sigma_z(t_i)}{2} \right], \quad (37)$$

with $\phi \equiv \omega(t_3 - t_1)$.

Since the cavities are to be prepared in states with well-defined large photon numbers N_1 and N_2 [see Eqs. (12)–(14)], we have as a consequence of (35)

$$\gamma_j^2(t_i) \cong N_j, \quad j = 1, 2. \quad (38)$$

It is therefore useful to decompose the exponentials involving $\gamma_j(t_i)$ into their even and odd parts

$$\begin{aligned} \exp(ig_j T_j \gamma_j) &= \cos[g_j T_j (\gamma_j^2)^{1/2}] \\ &\quad + i \gamma_j \frac{\sin[g_j T_j (\gamma_j^2)^{1/2}]}{(\gamma_j^2)^{1/2}} \\ &\cong \cos(g_j T_j \sqrt{N_j}) + i \frac{\gamma_j}{\sqrt{N_j}} \sin(g_j T_j \sqrt{N_j}). \end{aligned} \quad (39)$$

In order to arrange for double spin flip, we require

$$\sin(g_j T_j \sqrt{N_j}) = 1 \quad \text{or} \quad g_j T_j \sqrt{N_j} = \frac{\pi}{2}, \quad (40)$$

which allows us to write

$$\begin{aligned} \frac{1 + \sigma_z}{2} \exp(ig_2 T_2 \gamma_2) \exp(ig_1 T_1 \gamma_1) &\cong \frac{1 + \sigma_z}{2} \frac{i \gamma_2}{\sqrt{N_2}} \frac{i \gamma_1}{\sqrt{N_1}} \\ &= -\frac{1 + \sigma_z}{2} \frac{a_2 a_1^\dagger}{\sqrt{N_1 N_2}}. \end{aligned} \quad (41)$$

The spin-photon part of $U = U_{\text{SGI}} U_{\sigma, a}$ is then given by

$$\begin{aligned} U_{\sigma, a}(t_i, t_f) &= \exp \left\{ -i \omega (t_f - t_i) (a_1^\dagger a_1 + a_2^\dagger a_2) \right. \\ &\quad \left. - \frac{i}{2} \phi \sigma_z \right\} \\ &\times \left[-\frac{1 + \sigma_z}{2} \frac{a_2 a_1^\dagger}{\sqrt{N_1 N_2}} + \frac{1 - \sigma_z}{2} \right], \end{aligned} \quad (42)$$

where all operators are at time t_i , or all at time t_f .

This $U_{\sigma,a}(t_i, t_f)$ is, of course, only to be used in connection with appropriately prepared cavity states. In particular, the atoms leaving the second cavity *must* be in spin-up states; otherwise, some fraction of them will be deflected in the wrong direction by the intended recombinating stage of the SGI. More generally put, the expectation value of σ_z at the final time t_f must equal that at the initial time t_i or

$$\begin{aligned} \langle \frac{1}{2}[1 + \sigma_z(t_i)] \rangle &= \langle \frac{1}{2}[1 + \sigma_z(t_f)] \rangle \\ &= \langle U_{\sigma,a}^{-1}(t_i, t_f) \frac{1}{2}[1 + \sigma_z(t_i)] U_{\sigma,a}(t_i, t_f) \rangle \\ &= \frac{1}{N_1 N_2} \langle a_1 a_2^\dagger \frac{1}{2}(1 + \sigma_z) a_2 a_1^\dagger \rangle, \end{aligned} \quad (43)$$

and we note that in the last expression all operators are at time t_i , when the various degrees of freedom σ, a_1, a_2 are not correlated. Thus

$$\begin{aligned} \langle \frac{1}{2}[1 + \sigma_z(t_f)] \rangle &= \left\langle \frac{1}{N_1 N_2} \langle a_1 a_1^\dagger \rangle \langle a_2^\dagger a_2 \rangle \langle \frac{1}{2}(1 + \sigma_z) \rangle \right\rangle_{t_i} \\ &= \langle \frac{1}{2}[1 + \sigma_z(t_i)] \rangle, \end{aligned} \quad (44)$$

as desired and required.

It is essential to appreciate that $N_{1,2}$ are really very large numbers. In connection with (27) we found that $\hbar g / \hbar \omega \sim 10^{-11}$, typically. Next, $\omega T = \omega L / v \sim c / v$; atoms driving masers move at a speed of about $v \sim 10^4$ cm/s, so that $\omega T \sim 10^6$. Thus, to realize (45), one needs

$$N_{1,2} \sim \left[\frac{1}{gT} \right]^2 = \left[\frac{\omega}{g} \frac{1}{\omega T} \right]^2 \sim (10^{11} \times 10^{-6})^2 = 10^{10} \quad (45)$$

photons.

It is appropriate to mention here that we are appealing to the micromaser techniques¹⁰ by which one can prepare the cavities in desired states, and the ability to choose initial number or coherent states is essential for the *welcher Weg* detector. Of course, we do not seriously suggest preparing a number state with 10^{10} photons. This is far beyond the experimentally achievable. Therefore, what we describe here is a gedanken experiment. Realistic experiments in the same spirit will be discussed elsewhere.¹¹

B. Final spin and photon measurements

As a first application of the effective evolution operator (42), needed in Eq. (10), consider $\langle \sigma_+(t_f) \rangle$. It is given by

$$\begin{aligned} \langle \sigma_+(t_f) \rangle &= \langle U_{\sigma,a}^{-1}(t_i, t_f) \sigma_+(t_i) U_{\sigma,a}(t_i, t_f) \rangle \\ &= - \frac{1}{\sqrt{N_1 N_2}} e^{i\phi} \langle a_1(t_i) a_2^\dagger(t_i) \sigma_+(t_i) \rangle \\ &= - \frac{e^{i\phi}}{\sqrt{N_1 N_2}} \langle a_1(t_i) \rangle \langle a_2^\dagger(t_i) \rangle \langle \sigma_+(t_i) \rangle, \end{aligned} \quad (46)$$

where the last equality expresses the absence of correlations at time t_i . Applied to a $\sigma'_x(t_i) = 1$ state, when $\langle \sigma_+(t_i) \rangle = 1$, this produces Eq. (11).

Similarly, we find

$$\begin{aligned} \langle a_1^\dagger(t_f) a_1(t_f) \rangle &= \left\langle \frac{1 + \sigma_z(t_i)}{2} \right\rangle \frac{1}{N_1} \langle [a_1(t_i) a_1^\dagger(t_i)]^2 \rangle \frac{1}{N_2} \langle a_2^\dagger(t_i) a_2(t_i) \rangle + \left\langle \frac{1 - \sigma_z(t_i)}{2} \right\rangle \langle a_1^\dagger(t_i) a_1(t_i) \rangle \\ &\cong \left\langle \frac{1 - \sigma_z(t_i)}{2} \right\rangle N_1 + \left\langle \frac{1 + \sigma_z(t_i)}{2} \right\rangle (N_1 + 1), \end{aligned} \quad (47)$$

which is the basis of Eq. (19).

The state of the spin-photon system, characterized by a set of quantum numbers (symbolized by $\{q'\}$) at the initial time t_i , is expressed in terms of states referring to measurements at the final time t_f by means of

$$|\{q'\}, t_i\rangle = U_{\sigma,a}(t_i, t_f) |\{q'\}, t_f\rangle, \quad (48)$$

where it is now useful to take the operators in (42) at time t_f . For number-state preparation, we have $\{q'\} = \{(a_1^\dagger a_1)', (a_2^\dagger a_2)', \sigma'_x\} = \{N_1, N_2, 1\}$. In conjunction with

$$|\sigma'_x = 1\rangle = \frac{1}{\sqrt{2}} (|\sigma'_z = 1\rangle + |\sigma'_z = -1\rangle) = \frac{1}{\sqrt{2}} (|\uparrow\rangle + |\downarrow\rangle), \quad (49)$$

Eq. (48) then yields (20) with $\beta = \omega(t_f - t_i)$. Likewise, when classical coherent states are prepared, that is

$$\{q'\} = \{a'_1, a'_2, \sigma'_x\} = \{\sqrt{N_1} e^{i\theta_1}, \sqrt{N_2} e^{i\theta_2}, 1\},$$

one obtains (21).

C. Density-operator analysis

The density operator for the spin degree of freedom is, at any time, given by

$$\rho_{\text{spin}}(t) = \frac{1}{2} [1 + \langle \sigma(t) \rangle \cdot \sigma], \quad (50)$$

which, presented as a 2×2 matrix referring to measurements of σ_z , reads

$$\rho_{\text{spin}} = \frac{1}{2} \begin{bmatrix} 1 + \langle \sigma_z(t) \rangle & \langle \sigma_-(t) \rangle \\ \langle \sigma_+(t) \rangle & 1 - \langle \sigma_z(t) \rangle \end{bmatrix}. \quad (51)$$

In particular, for our experimental setup, we find

$$\rho_{\text{spin}}(t_i) = \frac{1}{2} (1 + \sigma_x) = \frac{1}{2} \begin{bmatrix} 1 & 1 \\ 1 & 1 \end{bmatrix} \quad (52)$$

and, as implied by Eqs. (44) and (46),

$$\rho_{\text{spin}}(t_f) = \frac{1}{2} \begin{pmatrix} 1 & -e^{-i\phi} \langle a_1^\dagger(t_i) \rangle \langle a_2(t_i) \rangle / \sqrt{N_1 N_2} \\ -e^{i\phi} \langle a_1(t_i) \rangle \langle a_2^\dagger(t_i) \rangle / \sqrt{N_1 N_2} & 1 \end{pmatrix}. \quad (53)$$

If classical coherent states are prepared initially, this says

$$\begin{aligned} \rho_{\text{spin}}(t_f) &= \frac{1}{2} \begin{pmatrix} 1 & e^{-i\psi} \\ e^{i\psi} & 1 \end{pmatrix} \\ &= \frac{1}{2} (1 + \sigma_x \cos\psi + \sigma_y \sin\psi), \end{aligned} \quad (54)$$

where ψ is the angle of the net Larmor precession in Eq. (21). On the other hand, cavities prepared in number states lead to

$$\rho_{\text{spin}}(t_f) = \frac{1}{2} \begin{pmatrix} 1 & 0 \\ 0 & 1 \end{pmatrix} = \frac{1}{2}. \quad (55)$$

$$\rho_{\text{spin-photon}}(t_f) = \rho_{\text{spin}}(\sigma_z, -e^{-i\phi} a_1^\dagger a_2 \sigma_+ / \sqrt{N_1 N_2}, -e^{i\phi} a_1 a_2^\dagger \sigma_- / \sqrt{N_1 N_2}) \rho_1(e^{i\beta} a_1, e^{-i\beta} a_1^\dagger) \rho_2(e^{i\beta} a_2, e^{-i\beta} a_2^\dagger), \quad (57)$$

where $\beta = \omega(t_f - t_i)$ as in (20) [see after (49)]. For ρ_{spin} of (52), the spin-matrix version of (57) is

$$\rho_{\text{spin-photon}}(t_f) = \frac{1}{2} \begin{pmatrix} 1 & -e^{-i\phi} a_1^\dagger a_2 / \sqrt{N_1 N_2} \\ -e^{i\phi} a_1 a_2^\dagger / \sqrt{N_1 N_2} & 1 \end{pmatrix} \rho_1(e^{i\beta} a_1, e^{-i\beta} a_1^\dagger) \rho_2(e^{i\beta} a_2, e^{-i\beta} a_2^\dagger), \quad (58)$$

where tracing over the photon variables yields the final ρ_{spin} of (53).

If now ρ_1 and ρ_2 in (56) project to classical coherent states, (58) is equivalent to

$$\begin{aligned} \rho_{\text{spin-photon}}(t_f) &= \frac{1}{2} \begin{pmatrix} 1 & e^{-i\psi} \\ e^{i\psi} & 1 \end{pmatrix} \rho_1(e^{i\beta} a_1, e^{-i\beta} a_1^\dagger) \\ &\quad \times \rho_2(e^{i\beta} a_2, e^{-i\beta} a_2^\dagger). \end{aligned} \quad (59)$$

This is a product analogous to the one in (56), telling us that the spin and photon degrees of freedom are again uncorrelated at the final time. In contrast, such a factorization is not possible if ρ_1 and ρ_2 in (56) project to number states, indicating the correlations established by the interaction.

In general terms, this discussion teaches us that the addition of a detector requires broadening the quantum description of the system of interest (here, the spin degree

of freedom) to include the detector (here, the photon degrees of freedom), with the consequence that system-detector correlations are dynamically established. Then projecting onto the system subspace (achieved by tracing over the detector variables) will result in a loss of quantal coherence, provided the detector is properly functioning (here, number states are prepared initially). It is worth pointing out that the detector need not have a large number of (relevant) degrees of freedom.

For ψ an even multiple of π , the different physical contents of (54) and (55) are illustrated in Fig. 5. In order to see here how this loss of coherence results from correlations between the spin and photon degrees of freedom, consider the density operator of the joint spin-photon system. At the initial time t_i , these degrees of freedom are uncorrelated, so that the joint density operator is a product:

$$\rho_{\text{spin-photon}}(t_i) = \rho_{\text{spin}}(\sigma_z, \sigma_+, \sigma_-) \rho_1(a_1, a_1^\dagger) \rho_2(a_2, a_2^\dagger). \quad (56)$$

The unitary evolution operator $U_{\sigma, a}$ of (42) turns this into

of freedom) to include the detector (here, the photon degrees of freedom), with the consequence that system-detector correlations are dynamically established. Then projecting onto the system subspace (achieved by tracing over the detector variables) will result in a loss of quantal coherence, provided the detector is properly functioning (here, number states are prepared initially). It is worth pointing out that the detector need not have a large number of (relevant) degrees of freedom.

D. Neutron interferometer spin-flip measurements

In a series of experiments⁵ Rauch *et al.* have set up a neutron interferometer along the lines of an optical Twyman-Green interferometer. In these experiments they have observed the interference behavior associated with the neutron waves.

They then proceed to introduce radiation fields into the various arms of the interferometer so as to flip the neu-

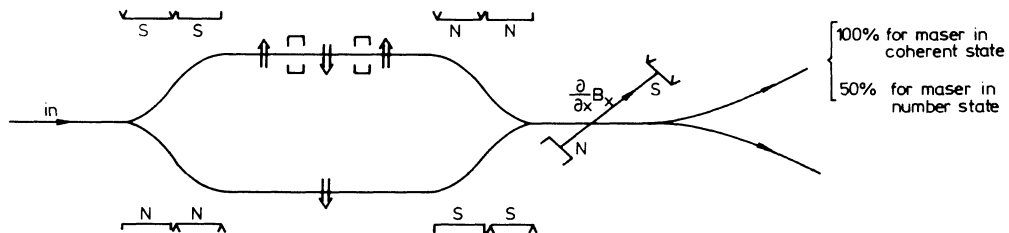


FIG. 5. SGI with micromasers and SGA for final σ_x measurements, comparing classical coherent states and number states.

tron spins. Concerning these experiments they say, "It is shown that under the given circumstances of neutron self-interference coherence is preserved, . . ." The important point, consistent with the present discussion, is that *the spin flip interaction with the coherent state radiation field does not destroy spin coherence.*

III. DISCUSSION

A. Summary

We have seen that the act of correlating our spin- $\frac{1}{2}$ atom with the detector can destroy the coherence in our spin system. But, how can this be? The atoms are really undergoing an up-down-up spin flip upon interaction with the microwave field. Superficially, one might think that this results in no net change to the spin system. Indeed, for classical coherent states of the maser fields, this is so. However, when number-state maser fields are used, spin coherence *is* destroyed—Humpty-Dumpty is broken for good.

The destruction of spin coherence in the micromaser fields does not arise because of recoil effects, as in the example of Sec. I B, rather it comes from the photon-spin correlations that have been established. We could count the number of photons in cavities 1 and 2 and tell whether a spin-up or a spin-down atom has passed through the SGI.

As an example of an experiment in which the results are influenced by the presence of the detection system consider the setup of Fig. 5, where a final SGA is present with a magnetic field along the x direction. When the cavity fields are prepared in coherent states [and the Larmor angle ψ appearing in (21) equals an even multiple of π] the entire beam will ideally be deflected in the $+x$ direction. If, however, the cavity fields are initially in number states, then only half of the atoms will be deflected in the $+x$ direction. Whatever recoil effects are

there, they are essentially the same in both situations, so that the destruction of coherence in the second situation cannot be attributed to momentum transfer.

B. Number-state preparation

It should be emphasized that the present analysis depends crucially on the preparation of a number state in (one of) the microwave cavities. But, one might argue, it is not feasible to produce a number state of the radiation field and so the above experiment can be nothing more than a gedanken experiment. However, several recent papers¹²⁻¹⁴ have presented schemes and experiments aimed at number-state generation. Of special interest to us is a recent paper showing that a number state can be prepared when the radiation builds up in a microwave cavity having an extremely high Q value.¹³ Such cavities are actually now available.

Specifically, we can envision producing pure number states as follows. Atoms in their excited state are injected into the cavity; after they leave the cavity, they are probed by a static electric field which ionizes all atoms in their upper level. The atoms that are not ionized have emitted a photon in the cavity; when these atoms are counted (via electron detection), the total number of photons in the maser field can be inferred. For further discussion concerning this point we refer the reader to Refs. 13 and 14.

ACKNOWLEDGMENTS

This work is supported by the U.S. Office of Naval Research, Department of the Navy (ONR). One or more of the authors wish to thank their colleagues for stimulating and productive discussions, including A. Barut, D. Greenberger, S. Haroche, W. Lamb, R. O'Connell, H. Rauch, H. Walter, E. Wigner, and A. Zeilinger.

APPENDIX

The evolution operator $U_{\text{eff}}(t', t)$ corresponding to the effective Hamilton operator (36) obeys the differential equation

$$i\hbar \frac{\partial}{\partial t} U_{\text{eff}}(t', t) = H_{\text{eff}}(t) U_{\text{eff}}(t', t), \quad (\text{A1})$$

subject to the initial condition $U_{\text{eff}}(t', t') = 1$. For $t_1 < t < t_2$, both γ_1 and $a_2^\dagger a_2$ are constants of the motion. So we find immediately

$$U_{\text{eff}}(t_1, t_2) = \exp\{-i\omega(t_2 - t_1)[\gamma_1^2(t_1) + a_2^\dagger(t_1)a_2(t_1) - \frac{1}{2}]\} \exp[ig_1 T_1 \gamma_1(t_1)]. \quad (\text{A2})$$

Likewise we have

$$\begin{aligned} U_{\text{eff}}(t_2, t_3) &= \exp\{-i\omega(t_3 - t_2)[a_1^\dagger(t_2)a_1(t_2) + \gamma_2^2(t_2) - \frac{1}{2}]\} \exp[ig_2 T_2 \gamma_2(t_2)] \\ &= U_{\text{eff}}^{-1}(t_1, t_2) \exp\{-i\omega(t_3 - t_2)[a_1^\dagger(t_1)a_1(t_1) + \gamma_2^2(t_1) - \frac{1}{2}]\} \exp[ig_2 T_2 \gamma_2(t_1)] U_{\text{eff}}(t_1, t_2). \end{aligned} \quad (\text{A3})$$

These are combined into

$$\begin{aligned} U_{\text{eff}}(t_1, t_3) &= U_{\text{eff}}(t_1, t_2) U_{\text{eff}}(t_2, t_3) = \exp[-i\omega(t_3 - t_2)(a_1^\dagger a_1 + \gamma_2^2 - \frac{1}{2})] \exp[ig_2 T_2 \gamma_2] \\ &\quad \times \exp[-i\omega(t_2 - t_1)(\gamma_1^2 + a_2^\dagger a_2 - \frac{1}{2})] \exp[ig_1 T_1 \gamma_1] \end{aligned} \quad (\text{A4})$$

or

$$U_{\text{eff}}(t_1, t_3) = \exp[-i\omega(t_3 - t_1)(a_1^\dagger a_1 + a_2^\dagger a_2 + \frac{1}{2}\sigma_z)] \exp[ig_2 T_2 \gamma_2] \exp[ig_1 T_1 \gamma_1], \quad (\text{A5})$$

where all operators are taken at time t_1 before the interaction.

This is the effective evolution operator to be used for the upper beam, the one for which $\sigma'_z(t_1)=1$. The corresponding U_{eff} for the lower beam with $\sigma'_z(t_1)=-1$ is obtained by setting $g_1=g_2=0$ in (A5) since this partial beam does not interact with the cavity modes. After identifying t_1 and t_3 with the instants when the atom enters and leaves the additional magnetic field \mathbf{B}_0 , we find the overall evolution operator of Eq. (9) to be given by [$\phi \equiv \omega(t_3 - t_1)$]

$$U(t_i, t_f) = U_{\text{SGI}}(t_i, t_f) \exp\{-i\omega(t_f - t_i)[a_1^\dagger(t_i)a_1(t_i) + a_2^\dagger(t_i)a_2(t_i)]\} \exp\left[-\frac{i}{2}\phi\sigma_z(t_i)\right] \\ \times \left[\frac{1+\sigma_z(t_i)}{2} \exp[ig_2 T_2 \gamma_2(t_i)] \exp[ig_1 T_1 \gamma_1(t_i)] + \frac{1-\sigma_z(t_i)}{2}\right]. \quad (\text{A6})$$

*Permanent address: Sektion Physik, Universität München, 8046 Garching, Federal Republic of Germany.

†Permanent address: Department of Physics, University of California, Los Angeles, CA 90024.

¹E. P. Wigner, *Am. J. Phys.* **31**, 6 (1963). The device is mentioned earlier by D. Bohm, *Quantum Theory* (Prentice-Hall, Englewood Cliffs, NJ, 1951).

²W. Gerlach and O. Stern, *Z. Phys.* **8**, 110 (1922); **9**, 349 (1922).

³B.-G. Englert, J. Schwinger, and M. O. Scully, *Found. Phys.* **18**, 1045 (1988). The original Humpty-Dumpty problem:

“Humpty-Dumpty sat on a wall, Humpty-Dumpty had a great fall; All the King’s horses and all the King’s men couldn’t put Humpty-Dumpty together again.”

(The Humpty-Dumpty rhyme is actually a riddle, with the solution: egg.)

⁴J. Schwinger, M. O. Scully, and B.-G. Englert, *Z. Phys. D* **10**, 135 (1988).

⁵G. Badurek, H. Rauch, and D. Tuppinger, *Phys. Rev. A* **34**, 2600 (1986); and earlier work cited therein.

⁶W. Heisenberg, *Die Physikalischen Prinzipien der Quantentheorie* (Hirzel, Leipzig, 1930).

⁷M. O. Scully, R. Shea, and J. D. McCullen, *Phys. Rep.* **43**, 485 (1978).

⁸Realistic experiments will have to use *electric* dipole interactions instead. Nevertheless, we present a detailed treatment of a magnetic coupling, because it avoids the introduction of additional internal atomic degrees of freedom.

⁹B.-G. Englert, J. Schwinger, and M. O. Scully (unpublished).

¹⁰D. Meschede, H. Walther, and G. Müller, *Phys. Rev. Lett.* **54**, 551 (1985); G. Rempe, H. Walther, and N. Klein, *ibid.* **58**, 353 (1987).

¹¹We have, only for the sake of simplicity, assumed that the

coupling of the atoms to the cavity photons is via the *magnetic* moment. It is, however, much more practical to have *electric* dipole coupling to a transition between two highly excited states (so-called Rydberg states). In the first cavity, for example, the transition from the higher to the lower one of these states would occur, to be reversed in the second one, so that the atom emerges in the same Rydberg state in which it was prepared and with the same orientation of the magnetic moment to ensure the focusing by the final section of the SGI. By using such Rydberg transitions, the coupling strength is increased by, roughly, a factor of 10^5 , whereby the required number of photons is reduced to $\sim 10^{10}/(10^5)^2=1$. The preparation of a number state with a few photons is feasible; see Sec. III B.

This also lends justification to the way in which we arrived at the *resonant* Hamiltonian (33). The additional homogeneous magnetic field was there taken to be the same inside the cavities and outside. For the high-quality cavities that are actually needed, with superconducting walls, this is—to say the least—far fetched. (Incidentally, for the typical numbers used above, resonance requires a field strength ~ 1 kG inside the cavities.) However, keeping in mind that a realistic experiment would use a Rydberg transition, the Hamiltonian (33) is fine if one understands that the σ operators therein do not refer to the spin degree of freedom but to the two-level system consisting of the two Rydberg states.

¹²P. Filipowicz, J. Javanainen, and P. Meystre, *J. Opt. Soc. Am. B* **3**, 906 (1986); M. Kitagawa and Y. Yamamoto, *Phys. Rev. A* **34**, 3974 (1986); P. Meystre, *Opt. Lett.* **12**, 669 (1987).

¹³J. Krause, M. O. Scully, and H. Walther, *Phys. Rev. A* **36**, 4547 (1987).

¹⁴J. Krause, M. O. Scully, T. Walther, and H. Walther, *Phys. Rev. A* **39**, 1915 (1989).